Proceedings of the ASME 2011 Pressure Vessels & Piping Division Conference
PVP2011
July 17-21, 2011, Baltimore, Maryland, USA

PVP2011-57554

SIMULATION OF LOW-REYNOLDS NUMBER FLOW AROUND AN OSCILLATED CYLINDER USING TWO COMPUTATIONAL METHODS

L§szl· Baranyi
Department of Fluid & Heat Engineering,
University of Miskolc
Miskolc, Hungary
arambl@uni-miskolc.hu

Betti Boll·
Department of Fluid & Heat Engineering,
University of Miskolc
Miskolc, Hungary
aramzb@uni-miskolc.hu

L§szl· Dar· czy
University of Miskolc
Miskolc, Hungary
daroczy4@freemail.hu

ABSTRACT

The two-dimensional flow around a circular cylinder oscillated in-line and transverse to the main stream at low Reynolds numbers is investigated numerically using a 2D in-house code (Baranyi, 2008) based on a finite difference solution (FDM). A second CFD approach, the commercial software FLUENT based on the finite volume method (FVM), uses equivalent oscillatory flow to perform computations for the same conditions. Here we investigate the Reynolds numbers of Re=100, 120, 140 and 160 using two computational domains characterized by R_2/R_1=60 and 360. Computations are carried out at two frequency ratios of f/St_0=0.8 and 0.9 for different oscillation amplitude values in the lock-in domain. Both methods analyze flow properties such as drag, lift and mechanical energy transfer between the fluid and the cylinder for both transverse and in-line cylinder motions. Computational results obtained using the two methods for both type of cylinder motions agree well.

Keywords: circular cylinder, in-line oscillation, mechanical energy transfer, oscillatory flow, transverse oscillation

INTRODUCTION

The flow around oscillating bluff bodies is an important engineering problem. Examples are chimney stacks, cables of suspended bridges, offshore structures and risers, and transmission lines, which are exposed to wind or ocean currents. Despite its simple geometry, flow past an oscillating circular cylinder is considered to be a baseline case for more complex cases. Topics relevant to the current study are forced in-line and transverse cylinder oscillation in a uniform stream and oscillatory flow. Of the numerous studies in these areas, we would like to mention just a few.

For forced transverse cylinder motion one landmark study is that of Williamson and Roshko (1988) in which they created their well-known map of vortex synchronization regions for Re=392. Lu and Dalton (1996), Blackburn and Henderson (1999), and Kaiktsis et al. (2007) all found switches in the vortex structure for forced transverse cylinder motion when changing the frequency ratio at Reynolds numbers ranging from 185 to 1000. Zheng and Zhang (2008) looked at subharmonic and superharmonic forced cylinder oscillation in transverse direction at Re=200 using the immersed-boundary method, investigating frequency and amplitude effects. Didier and Borges (2007) carried out a systematic evaluation of transverse and in-line oscillation for low Reynolds numbers over a wide frequency domain.

For in-line forced cylinder oscillation, studies include Cetiner and Rockwell (2001), who investigated experimentally over a wide frequency ratio and at medium Re; Al-Mdallal et al. (2007) with a numerical study at Re=200 over a wide frequency ratio, who found vortex switches; and a mathematical model developed by Mureithi et al. (2010) for the investigation of dynamical bifurcation behavior.

Oscillatory flow has been investigated, for instance, experimentally and numerically by Bearman and Graham (1980) and numerically in Meneghini and Bearman (1995). The experimental study of Konstantinidis and Balabani (2007) perturbed the inflow by periodic oscillation and found that the symmetric vortex arrangement is not stable.

The main objective of the present study is to compare results from two very different CFD methods in order to further

support previous findings (Baranyi, 2009, and Baranyi et al., 2010). The first author used his own finite difference method (FDM) code using boundary-fitted coordinates. The second author used the commercial software FLUENT, based on the finite volume method (FVM). Both methods analyze flow properties such as drag, lift and torque coefficients, and mechanical energy transfer between the fluid and the cylinder. The effect of oscillation amplitude on the flow around a circular cylinder oscillating transverse and in-line is investigated at four different low Reynolds numbers and at two frequency ratios.

NOMENCLATURE

$a_{0x,y}$ the dimensionless x and y components of cylinder acceleration
$A_{x,y}$ amplitude of oscillation in x or y directions, respectively, non-dimensionalized by d
C_D drag coefficient, $2F_D/(\rho U^2 d)$
C_L lift coefficient, $2F_L/(\rho U^2 d)$
d cylinder diameter (m)
E mechanical energy transfer
f oscillation frequency, non-dimensionalized by U/d
f_v vortex shedding frequency, non-dimensionalized by U/d
R radius, non-dimensionalized by d
Re Reynolds number, Ud/n
St non-dimensional vortex shedding frequency, $f_v d/U$
t time, non-dimensionalized by d/U
tq torque coefficient, torque of shear on cylinder surface, non-dimensionalized by $\rho U^2 d^2$
U free stream velocity, velocity scale (m/s)
x,y Cartesian coordinates, non-dimensionalized by d
θ angle between resultant force and drag

Subscripts

D drag
fb fixed body
L lift
rms root-mean-square value
v vortex shedding
x, y components in x and y directions
0 for cylinder motion; for stationary cylinder at same Re
1 on the cylinder surface; for energy transfer in transverse direction
2 on the outer boundary of the physical domain; for energy transfer in in-line direction

COMPUTATIONAL METHODS

For the 2D in-house FDM code a non-inertial system fixed to the cylinder is used to compute two-dimensional low-Reynolds number unsteady flow around a circular cylinder placed in a uniform stream and forced to oscillate in in-line or transverse directions. The governing equations are the non-dimensional Navier-Stokes equations for incompressible constant-property Newtonian fluid, the equation of continuity and the Poisson equation for pressure. On the cylinder surface, no-slip boundary condition is used for the velocity and a Neumann type boundary condition is used for the pressure. Potential flow is assumed as an initial condition except for the cylinder surface, where zero velocity is used. For further details see Baranyi (2008).

FVM simulations were carried out using FLUENT v6.3.26 commercial software. The 2D, unsteady, laminar, segregated solver is used to solve the incompressible oscillatory flow for the collocated grid arrangement. The second order upwind scheme was used to discretize the convective terms in the momentum equations. The semi-implicit method for the pressure linked equations (SIMPLE) scheme is applied for solving the pressure-velocity coupling.

For both methods the computational domain is characterized by two concentric circles: the inner represents the cylinder surface with radius R_1, the outer the far field with radius R_2. The origin of the coordinate system is in the centre of the cylinder. The positive x axis is directed downstream. The computational domain size is R_2/R_1=60 and 360 with corresponding mesh points of 361x236 and 481x451 (azimuthal x radial), respectively. In the physical domain logarithmically spaced radial cells are used, providing a fine grid scale near the cylinder wall and a coarse grid in the far field. A dimensionless time step of t=0.0005 is used for the FDM, and t=0.001 for the FVM.

Both methods have been extensively tested against experimental and computational results (see Baranyi, 2008 and Bolló and Baranyi, 2010) and very good agreements were found for both methods.

The FDM code is set up for a mechanically-oscillated cylinder placed in a uniform stream U, while the FVM simulation is for oscillatory flow around a stationary cylinder. However, when viewed from a system fixed to the cylinder, these two cases are kinematically identical (though dynamically not) and can thus be compared. The non-dimensional cylinder displacement of the centre of the cylinder is described by

$$x_0(t) = A_x \cos(2p\ f_x t),\ y_0(t) = -A_y \sin(2p\ f_y t), \qquad (1)$$

where t is the non-dimensional time, and f_x, f_y and A_x, A_y are the non-dimensional amplitudes and frequencies of oscillation for in-line and transverse cylinder motions.

The non-dimensional frequency of oscillation $f = f_x = f_y$ was set at $0.8St_0$ and $0.9St_0$, where St_0 is the non-dimensional vortex shedding frequency, or Strouhal number, for a stationary cylinder at that Reynolds number. These frequency ratio values ensure that lock-in condition could be reached at moderate amplitude values. The flow was considered to be locked-in when the vortex shedding frequency f_v is equal to the frequency of cylinder oscillation f. For in-line oscillation, lock-in was found earlier in the vicinity of the natural vortex shedding frequency f_v (Baranyi, 2008), as well as the double of this frequency (Didier and Borges, 2007); here, subharmonic

frequency of oscillation is investigated. Only locked-in cases were considered in this study.

Time-mean (TM) and root-mean-square (rms) values of lift C_L, drag C_D, and torque tq coefficients were evaluated and plotted against the oscillation amplitude. Unless otherwise indicated the lift and drag coefficients shown in this study do not contain inertial forces (originating from the system fixed to the accelerating cylinder). Coefficients obtained by removing the inertial forces are often termed 'fixed body' coefficients (Lu and Dalton, 1996). The relationship between the two sets of coefficients can be written as

$$C_L = C_{Lfb} + \frac{\pi}{2} a_{0y}, \; C_D = C_{Dfb} + \frac{p}{2} a_{0x}, \qquad (2)$$

where subscript *fb* refers to the fixed body (understood in an inertial system fixed to the stationary cylinder) (Baranyi, 2005). Here a_{0x} and a_{0y} are the dimensionless x and y components of cylinder acceleration. Since these accelerations are periodic their time-mean values vanish, resulting in identical TM values for the two setups. Equation (2) shows that for in-line motion the two lift coefficients are identical, and the drag coefficients are different from each other. For transverse cylinder motion it is exactly the other way round.

The torque coefficient tq (positive in counter-clockwise direction) is non-dimensional torque originating from the shear stress acting on the cylinder surface (Baranyi, 2010). A similar torque coefficient is defined in Chen et al. (1995).

RESULTS

In the present study, computations for a cylinder oscillated mechanically in in-line and transverse direction were carried out at two frequency ratios and at Reynolds numbers of Re=100, 120, 140, and 160. For in-line motion we focus on the effects of oscillation amplitude at one fixed frequency, and for transverse motion we investigate oscillation amplitude effects on the rms and TM of force coefficients at two frequency ratios. The mechanical energy transfer between the fluid and the cylinder is analyzed for both motions.

In-line Cylinder Oscillation

Computations are performed at two Reynolds numbers (Re=100 and 120) and f=0.8St$_0$ values with amplitude of oscillation as the independent variable. For in-line motion only the larger domain (R_2/R_1=360) was used.

Figure 1 shows the TM of lift (and the identical fixed body lift) against the oscillation amplitude for FDM and FVM results at Re=100 and 120. As can be seen in the figure, the solution jumps between two states, as was found earlier by Baranyi (2009) and Baranyi et al. (2010). The state curves compare well for the two methods for both Reynolds numbers but the location and number of jumps are different. Experimental observations also show that the jump in phase for the lift is relatively independent of the Strouhal number and oscillation frequency but the magnitude of jump is not (Lei and Mian, 2010). As can also be seen in the figure, the two state curves are mirror images of each other, as was found earlier when several other forced in-line oscillation cases were investigated (Baranyi et al., 2010). Comparing Fig. 1(a) and Fig. 1(b), it can be seen that the lower boundary of the locked-in domain shifts towards smaller amplitude values with increasing Reynolds number. A more detailed investigation was presented in Baranyi et al. (2010) for in-line cylinder motion using the in-house FDM code used here, including nine Reynolds numbers ranging from 60 to 350 and two frequency ratios of f/St$_0$=0.8 and 0.9. In accordance with the results shown in Fig. 1, it was found that at both frequency ratios the symmetric state curves form "barrel-shape" for Re=120 and above and the state curves remain monotonic functions of amplitude A_x and the upper side of the barrel-shape is not realized in the lock-in domain.

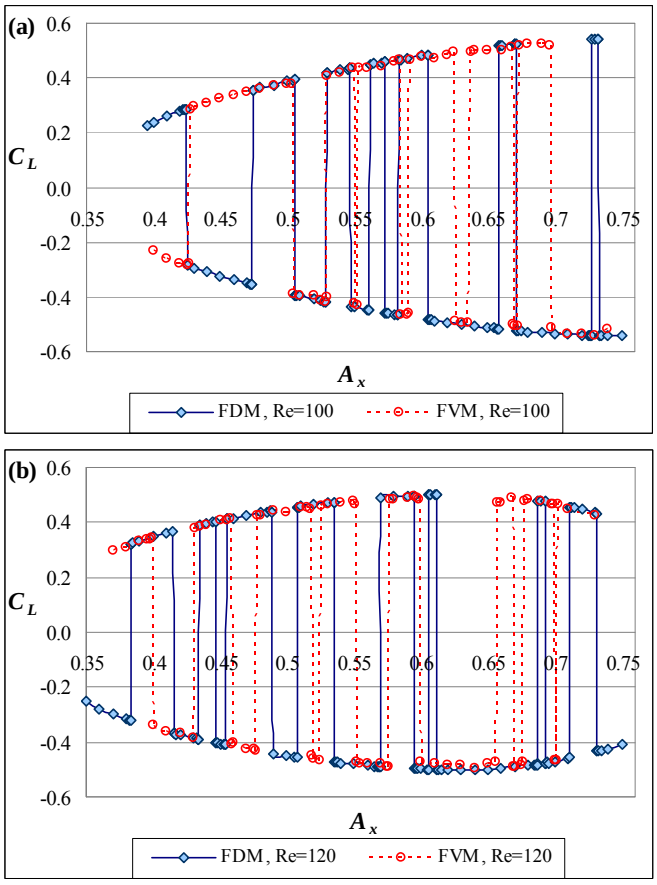

Figure 1. Time-mean value of lift versus amplitude at (a) Re=100 and (b) 120, using two CFD methods

The TM of torque is shown in Fig. 2 at (a) Re=100 and (b) Re=120. Although the discrepancy between the state curves predicted by the two methods for torque is a little larger than that for the TM of lift, basically the same conclusions can be drawn from this figure as from Fig. 1.

In agreement with the findings of Baranyi (2009) for in-line cylinder motion, two different state curves are found for the TM

of lift and torque, but a single state curve for the TM of drag and for all three (C_L, C_D and tq) rms curves. The TM of drag coefficient (identical with the TM of fixed body drag) is shown in Fig. 3 for both Re=100 and 120. Results obtained by FDM and FVM are again in good agreement. The TM of drag for Re=120 is larger than for Re=100 over almost the entire amplitude domain investigated. Naturally the drag increases with increasing amplitude values. As can be seen, the lower boundary of the lock-in domain shifts towards smaller amplitude values with increasing Reynolds number, similarly to the findings of Baranyi et al. (2010).

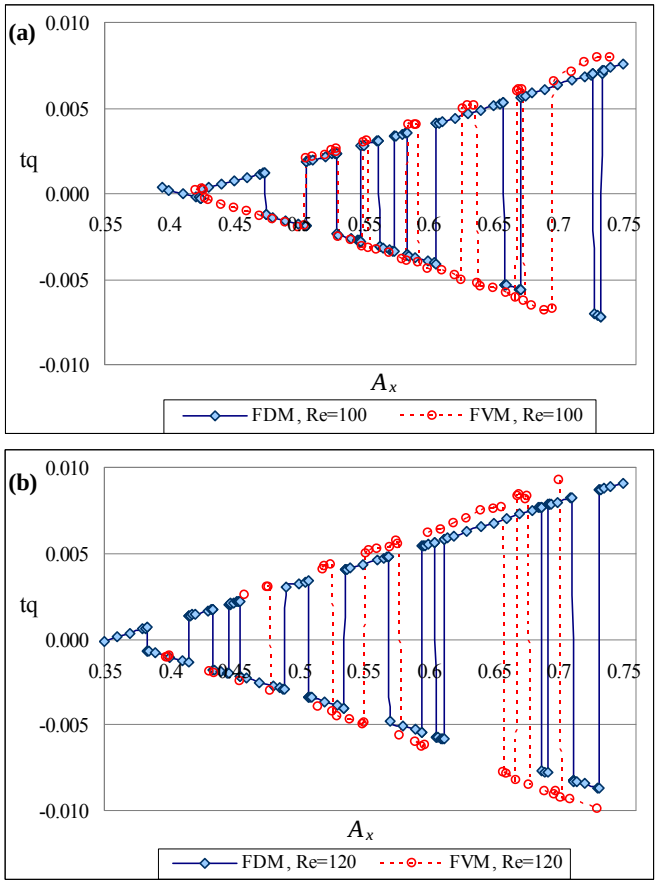

Figure 2. Time-mean value of torque versus amplitude at (a) Re=100 and (b) 120

The rms of the lift coefficient (identical with the rms of fixed body lift) is shown in Fig. 4. The two methods compare well again. As expected, the rms values increase with increasing amplitude, and the rms curve for Re=120 is above that for Re=100. The lower boundary of the lock-in domain shifts to lower amplitudes at the higher Reynolds number, as shown earlier for lift and drag in Baranyi et al. (2010).

The total load acting on a circular cylinder can be characterized by the resultant of lift and drag. It is also important to know the angle between the resultant force and drag at maximum lift and drag θ_{max}:

$$\theta_{max} = tan^{-1}\left(\frac{C_{Lmax}}{C_{Dmax}}\right), \qquad (3)$$

where C_{Lmax} and C_{Dmax} are maximal values of lift and drag. This is similar to the method employed by Lei and Mian (2010), who defined this angle for the maximum resultant. Since they were investigating much larger Reynolds numbers, however, results cannot be compared.

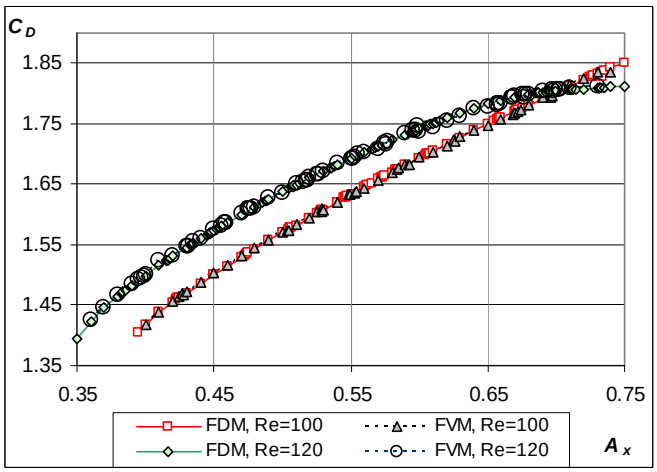

Figure 3. Time-mean value of drag versus amplitude at Re=100 and 120

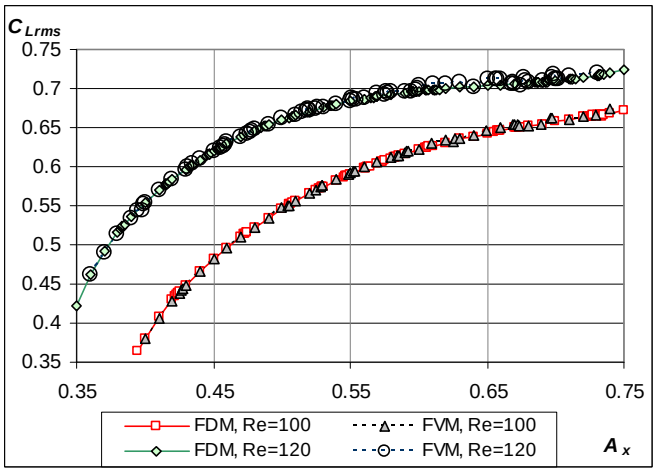

Figure 4. Rms value of lift versus amplitude at Re=100 and 120

Figure 5 shows FVM results at Re=100 for θ_{max} against oscillation amplitude. In addition, it compares the angle between drag and resultant force θ based on TM of lift and drag, for FVM and FDM computations. It can be seen that the θ values for both methods have identical state curves, though the number and location of jumps differ. Comparing θ and θ_{max}

once again two states are evident, and the location and number of jumps are identical.

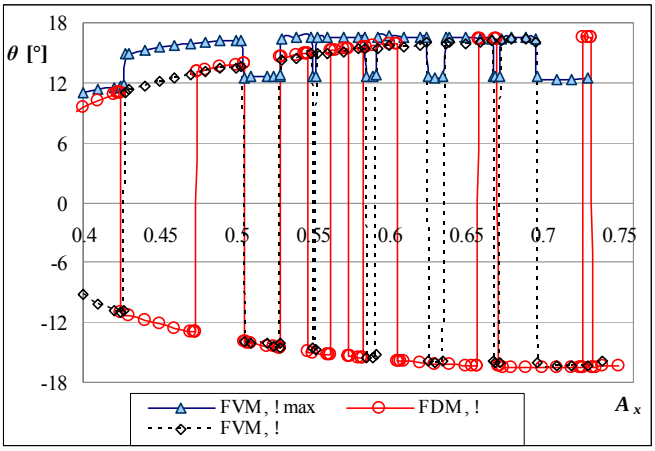

Figure 5. Angle between drag and resultant force versus amplitude at Re=100, based on maximum and on TM values of lift and drag

Pre- and Post Jump Analysis Let us investigate now the vicinity of a jump for both computational methods. Limit cycle curves (C_D,C_L) are shown for Re=100. As mentioned earlier, the location and number of jumps are different in the two methods. We have chosen here for comparison two jumps that are very near to each other. Then two points were selected: one in front, and one after the jump.

The limit cycle curve (x_0/A_x,C_L) is shown in Fig. 7(a) (for FDM) and in Fig. 7(b) (for FVM) for the pre- and post-jump for the same amplitude values as before. Again the pre-jump curve (thin line) is a mirror image of the post-jump curve (thick line). Before the jump the limit cycle curve is oriented in counterclockwise direction and TM lift coefficient is negative. After the jump the orientation of the limit cycle curve reverses and the TM of C_L becomes positive. The results of both methods agree well.

The vorticity contours shown in Fig. 8, belonging to the rightmost cylinder position, also show the mirror image of the flow before and after a jump for in-line cylinder motion (FDM). The gray indicates negative vorticity values, while the black is positive.

Figure 9 shows a periodic section of the time-history of lift at the amplitude of A_{x2}=0.5293, which is a pre-jump value for FVM and a post-jump value for FDM. The curves appear to be mirror images of each other.

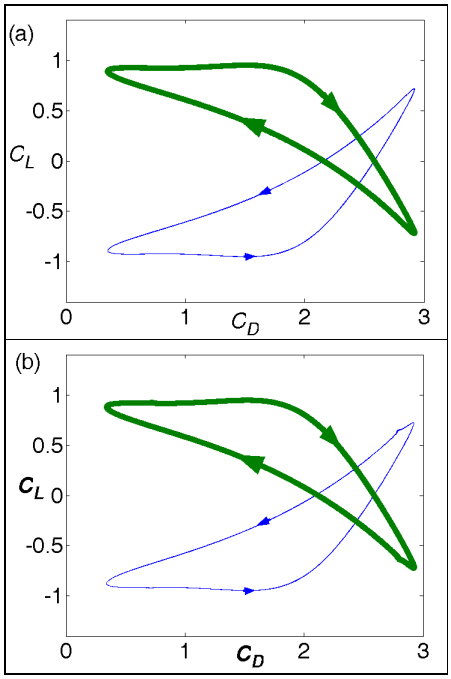

Figure 6. Limit cycle (C_D,C_L); Re=100
(a) FDM - thin line: A_x=0.529, thick line: A_x=0.5293
(b) FVM - thin line: A_x=0.5293, thick line: A_x=0.53

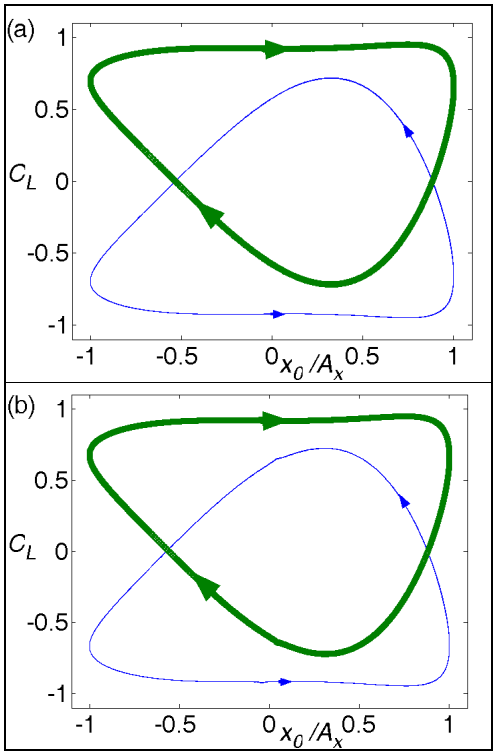

Figure 7. Limit cycles (x_0/A_x,C_L); Re=100
a) FDM - thin line: A_x=0.529, thick line: A_x=0.5293
b) FVM - thin line: A_x=0.5293, thick line: A_x=0.53

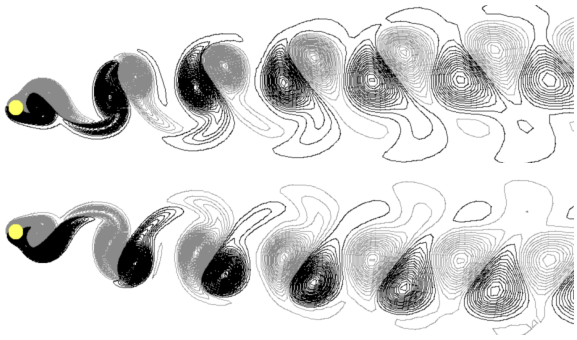

Figure 8. Vorticity contours: top A_x=0.529; bottom: A_x=0.5293; rightmost cylinder position in-line motion (Re=100; f_x=0.8St$_0$)

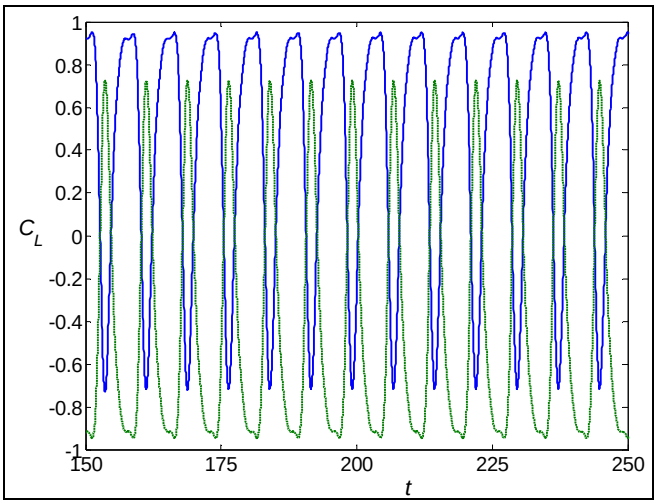

Figure 9. Time history of lift (solid line: FDM; dotted line: FVM) at A_x=0.5293; Re=100

Transverse Oscillation

The non-dimensional cylinder displacement of the centre of the cylinder for a transverse cylinder motion is obtained from Eq. (1) in the limiting case when the in-line amplitude A_x tends to zero. For this case, when TM and rms values of lift, drag and torque are plotted against A_y, no jumps were found in any of the curves, see Baranyi (2009).

Both methods analyzed the drag and lift coefficient at the two domain sizes of R_2/R_1=60 and 360 for different oscillation amplitude values in the lock-in domain at f/St$_0$=0.9 at Re=160. Figure 10 shows the TM of drag obtained by FDM and FVM for both domain sizes, and the rms of fixed body lift coefficient is shown in Fig. 11. As can be seen, the larger domain size yields slightly lower values for the TM of drag, as was also found in Anagnostopoulos and Minear (2004). The effect on the rms of lift is negligible. The slight difference between the results from the two domains in Figs. 10 and 11 may be partially attributed to the fact that the value of the Strouhal number is slightly different: St$_0$=0.1882 was found for R_2/R_1=60 during an earlier computation (Bolló and Baranyi, 2010) and in this study we found St$_0$=0.1864 for R_2/R_1=360. As can be seen in Figs. 10 and 11 both the TM of drag and the rms of lift increases almost linearly with increasing amplitudes. Designers of structures have to take into account the strong dependence of these parameters on the vibration amplitude. The two CFD methods yield practically the same results for both domain sizes.

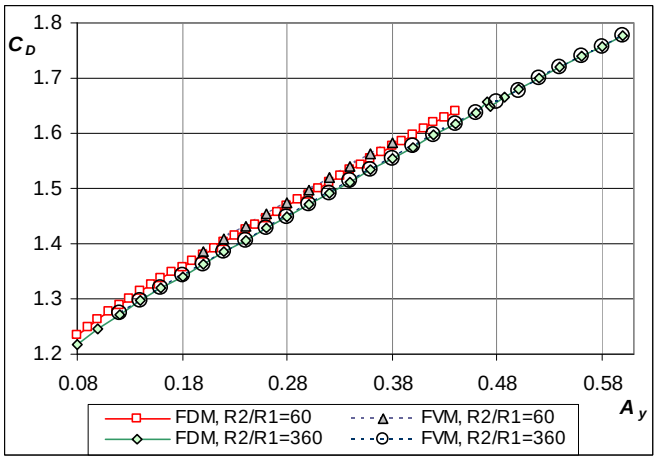

Figure 10. Time-mean of drag versus amplitude at R_2/R_1=60 and 360; Re=160; f/St$_0$=0.9

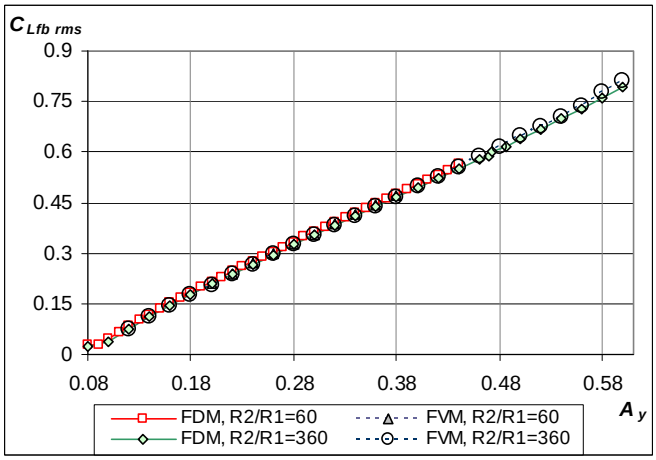

Figure 11. Rms of lift versus amplitude at R_2/R_1=60 and 360; Re=160; f/St$_0$=0.9

Computations were repeated for Re=140 for the smaller computational domain at f/St$_0$=0.9 against a series of transverse oscillation amplitudes and the results were compared for the corresponding case of Re=160. When plotted against oscillation amplitude the TM and rms drag curves values practically coincide with each other (not shown here) for the two Reynolds numbers. The rms values of fixed body lift are somewhat higher for Re=160 than those of for Re=140, though, as shown in Fig.

12. It can also be seen in the figure that C_{Lfbrms} almost linearly increases with increasing amplitude, and that the agreement between FDM and FVM results is very good.

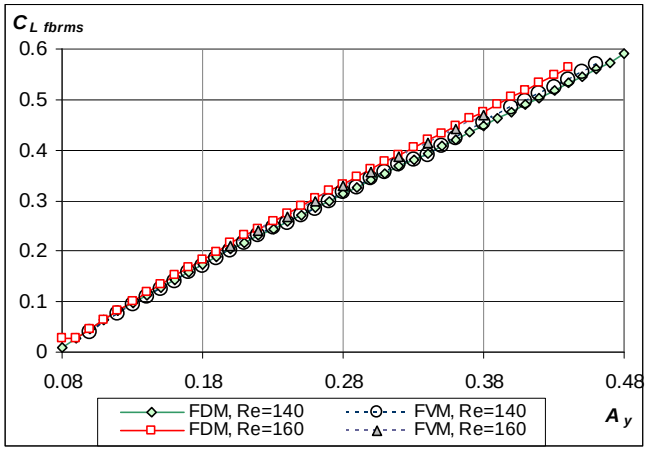

Figure 12. Rms of fixed body lift versus amplitude at Re=140 and 160 at R_2/R_1=60; f/St_0=0.9

Computations were also repeated for Re=160 over the larger computational domain at frequency ratio f/St_0=0.8. Figure 13 shows rms of fixed body lift versus amplitude for Re=160 at f/St_0=0.8 and 0.9. As can be seen, the agreement between the curves based on the results of the two methods is excellent for both frequency ratios. The slope of the rms curve for f/St_0=0.9 is larger than that for 0.8. The two curves intersect each other at about A_y=0.16, and above this amplitude value the distance between the two curves increases with increasing amplitude.

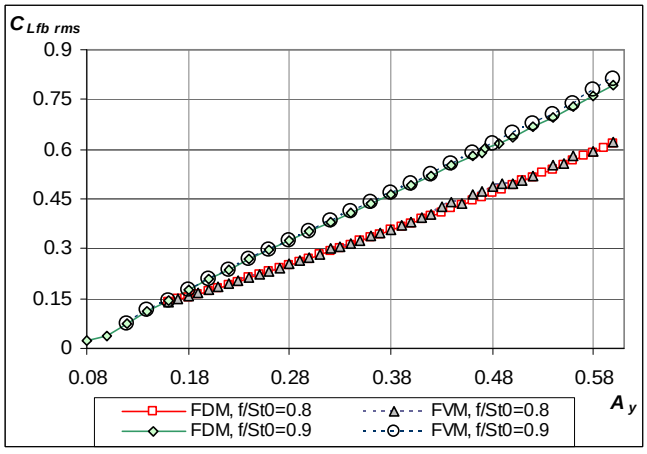

Figure 13. Rms of lift versus amplitude at f=0.8St$_0$ and 0.9St$_0$; Re=160; R_2/R_1=360

The TM of drag is shown against amplitude A_y in Fig. 14 for the frequency ratios of f/St_0=0.8 and 0.9 at Re=160. Again, excellent agreement is found between the two methods. The relationship between the TM of drag and amplitude is almost linear for both frequency ratios, and at any given amplitude the TM of drag is higher for the higher frequency ratio of 0.9.

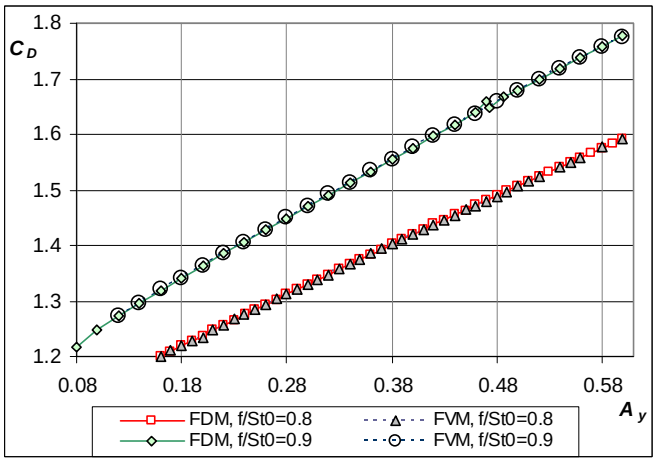

Figure 14. Time-mean of drag versus amplitude at f=0.8St$_0$ and 0.9St$_0$; Re=160; R_2/R_1=360

Mechanical Energy Transfer

The mechanical energy transfer between the fluid and the cylinder for transverse motions was defined in Blackburn and Henderson (1999) and it was extended for two-degree-of-freedom cylinder motion by Baranyi (2008). The total energy transfer E can be divided into two parts,

$$E = E_1 + E_2 , \tag{4}$$

where E_1 and E_2 are the energy transfer coefficients for transverse and in-line motion and can be written as follows:

$$E_1 = \int_0^T C_L(t)\dot{y}_0(t)dt , \; E_2 = \int_0^T C_D(t)\dot{x}_0(t)dt , \tag{5}$$

where T is the motion period, x_0 and y_0 represent the dimensionless displacement of the cylinder in x and y directions, respectively. The over dot means differentiation by dimensionless time. As seen in Eq. (5) for in-line cylinder motion E_1 is zero, so E=E_2; for transverse motion E_2 is zero, so E=E_1. For a general 2-DoF motion neither E_1 nor E_2 are zero and the total mechanical energy transfer is E=E_1+E_2.

Figure 15 shows the mechanical energy transfer E for in-line oscillation (E=E_2, see Eq. (5)) at Re=100, 120 and 160 at the frequency ratio of f/St_0=0.8 against oscillation amplitude A_x. The mechanical energy transfer for a cylinder oscillating in in-line direction was found to be always negative in the lock-in domain investigated. This means that the fluid acts against the cylinder motion, with a dampening effect. When the Reynolds number and frequency ratio are held constant, the absolute value of E increases with amplitude. In general, Reynolds number has little effect on energy transfer for in-line motion. However, at higher amplitude values, curves of Re=100 and

120 diverge slightly, as can be seen in the enlarged section of Fig. 15; for Re=120 the absolute value of energy transfer is lower than for Re=100. Predictions from the two methods compare well across the investigated domain.

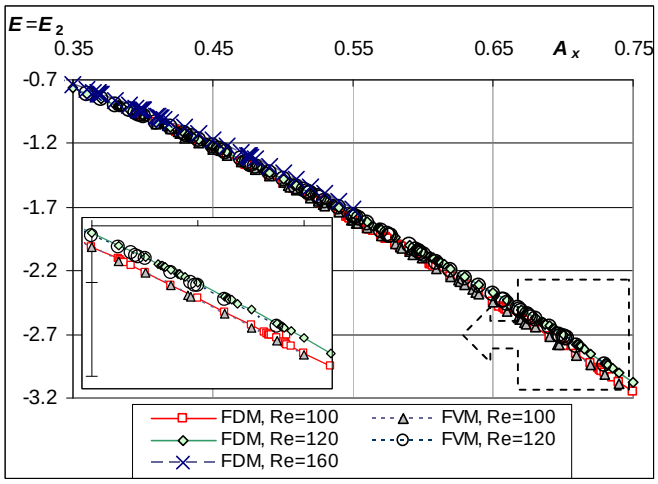

Figure 15. Mechanical energy transfer versus amplitude for in-line motion at Re=100, 120 and 160; f/St0=0.8

The energy transfer between the fluid and the body was also investigated for transverse cylinder oscillation. Figure 16 shows energy transfer $E=E_1$ at Re=160 for f/St_0=0.8 and 0.9 for both FDM and FVM. The mechanical energy transfer between the fluid and the cylinder first increases and then steeply decreases with increasing amplitude values. The value of energy transfer E can be either positive or negative as a function of oscillation amplitude. The energy transfer curve for the higher frequency ratio is positive for a larger range of amplitude A_y. Positive E values mean that energy is added to the cylinder from the fluid, and so flow-induced vibration is liable to occur. The two methods yield good agreement.

Figure 17 shows the lift coefficient versus the dimensionless displacement of the cylinder in y direction for four different amplitudes at Re=160 and at f/St_0=0.9 using FVM data. The area enclosed by the limit cycles ($\dot{y}_0, C_L$) represents the mechanical energy transfer $E=E_1$ (see Blackburn and Henderson, 1999; Baranyi, 2008). As can be seen in the figure, with increasing amplitude shape of area varies and the initial ellipse deforms. E is positive when the orientation of the limit cycle curves is clockwise (A_y=0.1 and 0.3), and E is negative when the orientation of the limit cycle curves is counterclockwise (A_y=0.50 and 0.58).

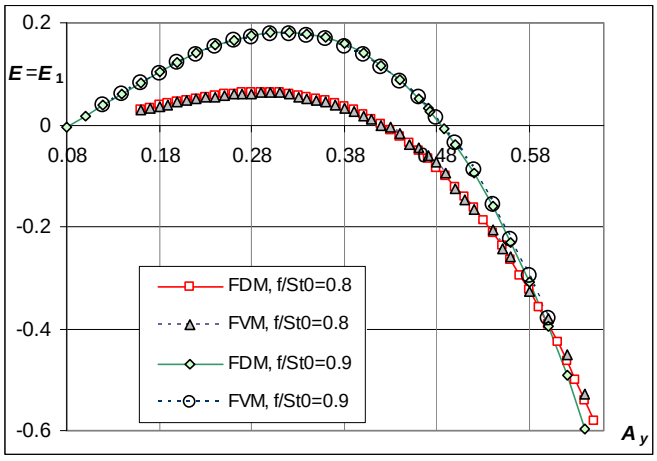

Figure 16. Mechanical energy transfer versus amplitude for transverse motion at f/St_0=0.8 and 0.9; Re=160

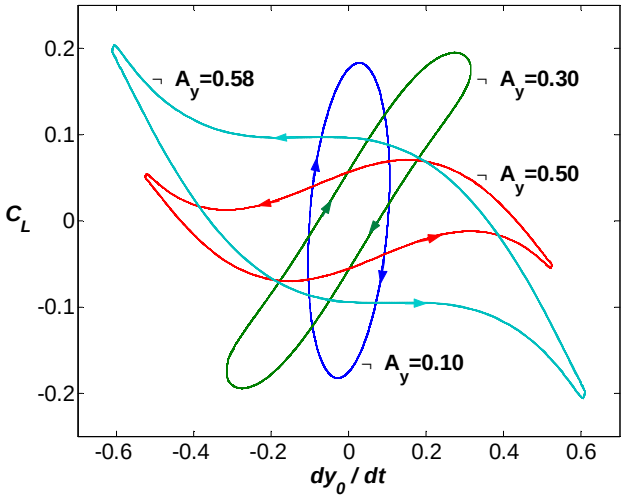

Figure 17. Limit cycles ($\dot{y}_0, C_L$) for transverse motion A_y=0.10, 0.30, 0.50, 0.58; f=0.9St_0; Re=160

CONCLUSIONS

Finite difference and finite volume methods were used to compute low Reynolds number 2D flow past an oscillating cylinder and an equivalent oscillatory flow. Computational results obtained using the two methods for in-line and transverse cylinder motions agree well.

In this study several computational aspects were investigated in order to ascertain whether the two methods give similar results for low-Reynolds flow.

- Reynolds number: Re=100, 120, 140 and 160, not much effect observed in transverse motion, larger in in-line motion cases. Larger Re shifts lock-in domain to smaller amplitude values.

- Computational domains, transverse motion: computations at R_2/R_1=60 and 360 showed minimal differences in results.
- Frequency ratio, transverse motion: f/St_0=0.8 and 0.9 curves of 0.9 fall above those of 0.8 and lock-in domain shifts towards smaller amplitude values.
- Energy transfer: for in-line motion results are always negative (flow acts against cylinder motion), while for transverse motion both positive (enhancing cylinder motion) and negative values occur.
- State curves, in-line motion: FDM and FVM yield the same state curves. Jumps between them appear in different locations and numbers.

The good agreement gained on all aspects investigated serves to act as supporting evidence for earlier findings from FDM studies (Baranyi, 2009; Baranyi et al., 2010). Further studies will include the investigation of flow at further Reynolds numbers and frequency ratios.

ACKNOWLEDGEMENTS

The support provided by the Hungarian Research Foundation (OTKA Projects K 76085 and K 68207) is gratefully acknowledged by the authors. The work was carried out as part of the TÁMOP-4.2.1.B-10/2/KONV-2010-0001 project in the framework of the New Hungarian Development Plan. The realization of this project is supported by the European Union, co-financed by the European Social Fund.

REFERENCES

Al-Mdallal, Q.M., Lawrence, K.P. and Kocabiyik, S., 2007, "Forced streamwise oscillations of a circular cylinder: Locked-on modes and resulting fluid forces," *Journal of Fluids and Structures* **23**, 681-701.

Anagnostopoulos, P. and Minear, R., 2004, "Blockage effect of oscillatory flow past a fixed cylinder," *Applied Ocean Research* **26**, 147–153.

Baranyi, L., 2005, "Lift and drag evaluation in translating and rotating non-inertial systems," *Journal of Fluids and Structures* **20**(1), 25-34.

Baranyi, L., 2008, "Numerical simulation of flow around an orbiting cylinder at different ellipticity values," *Journal of Fluids and Structures* **24**, 883-906.

Baranyi, L., 2009, "Sudden and gradual alteration of amplitude during the computation for flow around a cylinder oscillating in transverse or in-line direction," *ASME 2009 Pressure Vessels and Piping Conference*, *Symposium on Flow-Induced Vibration*. Prague, Paper No. PVP2009-77463.

Baranyi, L., Huynh, K. and Mureithi, N.W., 2010, "Dynamics of flow behind a cylinder oscillating in-line for low Reynolds numbers," Proc. *7th International Symposium on Fluid-Structure Interactions, Flow-Sound Interactions, and Flow-Induced Vibration and Noise*, Montreal, Québec, Canada, on CD ROM, pp. 1-10, Paper No. FEDSM-ICNMM2010-31183

Bearman, P.W. and Graham, J.M.R., 1980, "Vortex shedding from bluff bodies in oscillatory flow: A report on Euromech 119," *Journal of Fluid Mechanics* **99** (part 2), 225-245.

Blackburn, H.M. and Henderson, R.D., 1999, "A study of two-dimensional flow past an oscillating cylinder," *Journal of Fluid Mechanics* **385**, 255-286.

Bolló, B. and Baranyi, L., 2010, "Computation of low-Reynolds number flow around a stationary circular cylinder," *Proc. 7th International Conference on Mechanical Engineering*, Budapest, 891-896.

Cetiner, O. and Rockwell, D., 2001, "Streamwise oscillations of a cylinder in a steady current. Part 1. Locked-on states of vortex formation and loading," *Journal of Fluid Mechanics* **427**, 1-28.

Chen, M.M., Dalton, C. and Zhuang, L.X., 1995, "Force on a circular cylinder in an elliptical orbital flow at low Keulegan-Carpenter numbers," *Journal of Fluids and Structures* **9,** 617-638.

Didier, E. and Borges, A.R.J., 2007, "Numerical predictions of low Reynolds number flow over an oscillating circular cylinder," *Journal of Computational and Applied Mechanics* **8**(1), 39-55.

Kaiktsis, L., Triantafyllou, G.S. and Özbas, M., 2007, "Excitation, inertia, and drag forces on a cylinder vibrating transversely to a steady flow," *Journal of Fluids and Structures* **23**, 1-21.

Konstantinidis, E. and Balabani, S., 2007, "Symmetric vortex shedding in the near wake of a circular cylinder due to streamwise perturbations," *Journal of Fluids and Structures* **23**, 1047-1063.

Lei, L., Mian, L., 2010, "A numerical model for predicting the jump of lift force on an oscillating cylinder," *Ocean Engineering* **37**, 491–497.

Lu, X.Y. and Dalton, C., 1996, "Calculation of the timing of vortex formation from an oscillating cylinder," *Journal of Fluids and Structures* **10**, 527-541.

Meneghini, J.R. and Bearman, P.W., 1995, "Numerical simulation of high amplitude oscillatory flow about a circular cylinder," *Journal of Fluids and Structures* **9**, 435-455.

Mureithi, N.W., Huynh, K., Rodriguez, M. and Pham, A., (2010), "A simple low order model of forced Karman wake" *International Journal of Mechanical Sciences* **52**(11), 1522-1534.

Williamson, C.H.K. and Roshko, A., 1988, "Vortex formation in the wake of an oscillating cylinder," *Journal of Fluids and Structures* **2**, 355-381.

Zheng, Z.C. and Zhang, N., 2008, "Frequency effects on lift and drag for flow past an oscillating cylinder," *Journal of Fluids and Structures* **24**, 382-399.